Available online at www.sciencedirect.com
SCIENCE DIRECT®
Journal of Chromatography B, 800 (2004) 7–25
JOURNAL OF CHROMATOGRAPHY B
www.elsevier.com/locate/chromb

Review

Separation and analysis of colloidal/nano-particles including microorganisms by capillary electrophoresis: a fundamental review

Michael A. Rodriguez, Daniel W. Armstrong*

Department of Chemistry, Iowa State University, Ames, IA 50010, USA

Abstract

A review is presented on the CE analysis of colloidal/nano particles. Topics discussed include the CE separation of polymeric, inorganic, microbial (i.e. viruses, bacteria, fungi, and whole cells), and sub-cellular particles (i.e. mitochondria and nuclei). Several of the encountered difficulties in analysis are presented as well as the methods employed to overcome them.

Keywords: Reviews; Colloids; Nano-particles; Microbes

Contents

1. Introduction

Capillary electrokinetic separation methods have been used in several formats (i.e. capillary zone electrophoresis (CZE), capillary isoelectric focusing (CIEF), capillary isotachophoresis (CI), and capillary gel electrophoresis (CGE)) to analyze and characterize a wide variety of analytes from simple inorganic ions [1–3], small organic molecules [3], peptides [4,5], to proteins [4] DNA and RNA [6]. The fundamental factors governing the separation of these molecules have been understood for some time [7,8]. Movement occurs because charged species will move toward the direction of opposite charge when an electric field is applied. The solution around the molecule also imposes a frictional drag on the molecules as they move; therefore, the net mobility of a molecule (at equilibrium) is represented by the Eq. (1):

$$\mu = \frac{q}{f} \tag{1}$$

Abbreviations: CZE, capillary zone electrophoresis; CIEF, capillary isoelectric focusing; CI, capillary isotacophoresis; CGE, capillary gel electrophoresis; EH, electrophoretic heterogeneity; LDV, laser Doppler velocimetry; G6PDH, glucose-6-phosphate dehydrogenase; LIF, laser induced fluorescence; PSPs, polystyrene particles; CHAPS, 3-[(3-cholamidopropyl)dimethylammonio]propanesulfonic acid; PANI, polyaniline; PPy, polypyrrole; MPCs, monolayer protected gold clusters; $MEAV^{2+}(NO_3^-)_2$, *N*-(methyl)-*N*′-(ethylamine)-viologen dinitrate; TMV, tobacco mosaic virus; HRV, human rhinovirus; ACE, affinity capillary electrophoresis; VLDLs, very low density lipoprotein receptors; EOF, electroosmotic flow; TFFF, thermal field flow fractionation; MARK, microbe and radiolabel kinesis; DCIP, 2,6-dichlorophenolindophenol; FISH, fluorescence in situ hybridization; CCD, charge coupled device; FEP, fluorinated ethylene-propylene; G/R, green to red; ECC, electrokinetic capillary chromatography

* Corresponding author. Tel.: +1-515-294-1394; fax: +1-515-294-0838.
E-mail address: sec4dwa@iastate.edu (D.W. Armstrong).

1570-0232/$ – see front matter © 2003 Elsevier B.V. All rights reserved.
doi:10.1016/j.jchromb.2003.09.060

where μ is the electrophoretic mobility, q the net charge and f the translational friction coefficient (which is equal to $6\pi\eta R$, where R is the particle radius and η is viscosity). Often times the mobility is spoken of in terms of charge to size; however, it is understood that size relates directly to the frictional coefficient. This relationship was derived for spherical particles, which is a reasonable assumption unless very large molecules such as proteins, DNA and RNA are considered, then other models must be used [9]. These models still allow a fairly accurate prediction of the electrophoretic mobility. The reason CE is such an attractive technique for molecular analytes is because of the low sample consumption, fast analysis times, ease of automation and, of course, the extremely high efficiencies obtainable. In fact, for most of these analytes only a few factors contribute to the overall band broadening process, which enables the attainment of high efficiencies. The factors that contribute to total band broadening (σ_t^2) are indicated in Eq. (2):

$$\sigma_t^2 = \sigma_D^2 + \sigma_{\Delta T}^2 + \sigma_I^2 + \sigma_{det}^2 + \sigma_{\Delta\kappa}^2 + \sigma_{\Delta h}^2 + \sigma_W^2 + \sigma_{HD}^2 \quad (2)$$

where σ_D^2 represents the variance from longitudinal diffusion, $\sigma_{\Delta T}^2$ is the variance from the temperature profile, σ_I^2 is from the finite injection zone length, σ_{det}^2 is from finite detection width, $\sigma_{\Delta\kappa}^2$ is variance from conductivity differences, $\sigma_{\Delta h}^2$ is from siphoning effects, σ_W^2 from wall interactions, and σ_{HD}^2 is from hydrodynamic injection [10]. For inorganic ions, small organic molecules, and small peptides only the first three terms contribute significantly and cannot be controlled to a large extent by the operator. When working with large proteins or other macromolecules, the term from longitudinal diffusion can often be neglected, since they have diffusion coefficients much lower than those of small molecules. However, the band broadening term for wall interactions is often significant. In fact, under ideal conditions the Gaussian peak shape is the sole result of the distribution induced by longitudinal diffusion; therefore proteins, with minimal diffusion coefficients, would theoretically display a rectangular peak shape under these conditions (in reality, a situation quite difficult to produce). The fact that all entities of a particular molecular analyte are exactly identical to each other also simplifies matters. (This is not the case for colloidal analytes; the special problems they present will be discussed later.)

Recently, CE has been extended to include colloidal or nano-particles, which differ considerably from the aforementioned analytes. Colloidal particles typically have at least one dimension that ranges in size from the lower tens of nanometers to a few micrometers, while molecular sizes are usually expressed in terms of angstroms. A fundamental understanding of the electrophoretic process is more complicated for such particles. No longer can the relative electrophoretic mobility be estimated by considering the molecular weight and the expected charge. In fact, the molecular weights and overall charges are rarely known, unless measured beforehand by alternate techniques. These particles typically exhibit a wide distribution of charge, size, and shape; all of which can vary with experimental conditions and time. Frequently a single sample will have a distribution of properties and therefore electrophoretic mobilities. This quality is often referred to as electrophoretic heterogeneity (EH) [11]. This is not a problem when considering small molecular species or ions which are individually identical. The EH is an additional term that contributes to the total variance of the peak width in CE. Under conditions where all other sources of variance could be suppressed, EH alone would give rise to a broad and often irregular peak shape. The total variance from wall interactions can also be a problem for colloidal/nano particles. The potential for an enormous number of charges (if positive) and hydrophobic moieties on their surface can greatly increase the chance of wall interactions. In addition, the size of the particle itself and the fact that it is actually present as a heterogeneous solution increases the chance that it will physically contact the wall, which can sometimes retard its forward movement. In addition to the factors that affect variance, other factors that affect colloidal analysis are: particle–particle interactions and the stability of individual particles. Though molecules are constantly bombarding one another due to simple Brownian motion, this generally does not have an effect on their measured mobility or the mobility of other small molecular analytes in solution. This is not the case for colloidal particles, as sometimes the particles will adhere to each other once they come into contact, altering their mobility. This can also be a source of capillary clogging, if aggregation occurs to a large extent. In terms of stability, many biological colloids are susceptible to extremes of pH, osmolarity differences, or high electric fields, which can cause damage or rupture the structures. These are among a few of the factors affecting the analysis of colloidal particles by CE, many more exist. The aforementioned examples illustrate a few of the complicating factors that researchers in the field must deal with. This may explain why relatively little has been published in the area of colloidal or nano-particle CE, until recently.

Colloids such as polymeric particles (latex and others) are used in a number of different applications such as size standards [12], or immunoagglutination tests, where antibody coated polymer particles are an important part of the technique [13–15]. Inorganic colloidal particles have been extensively used in bioapplications such as DNA detection [16], immunospecific cell separations [17–19], and MRI contrast reagents [20]. The importance of biologically-related colloidal particles cannot be overstated; viruses, bacteria, and fungi, while important for pathological reasons, also provide antibiotics and vaccines. Structures such as liposomes have been used widely in the cosmetic industry, as drug delivery agents, and as model systems for many biological membranes [21]. Since these colloidal/nano particles are used in many ways and are important for a number of reasons, the careful characterization (in term of size and surface properties) of these particles is also essential. Techniques that

currently exist for the characterization of such particles are often very time consuming and complex. For instance, the size of inorganic and polymeric particles is typically characterized by laser light scattering, which is a notoriously difficult technique. The surface of these particles can be characterized by laser Doppler velocimetry (LDV), another complicated technique [22]. Biological characterization is typically performed by flow cytometry, which is very time consuming and prohibitively expensive. Surface characterization of these particles is done by microelectrophoresis, which is a labor intensive technique. CE is superior to these techniques because it can provide rapid information on both size and surface characteristics in a very simple manner. These are the main reasons why there has been an effort to extend CE to colloidal/nano analysis. Although CE may have initially appeared to be unsuitable for these types of analyses, researchers have made significant strides in developing CE as a very competitive technique for the analysis of particles. The aim of this review is to present the past and present findings on the CE analysis and characterization of colloidal/nano particles, including polymeric colloids, inorganic colloids, and biological colloids (viruses, bacteria, fungi, whole cells, and other cellular constituents). Another function of this review is to describe the ways in which various researchers have overcome the analytical difficulties initially presented by colloidal/nano-analytes.

2. CE of colloidal/nano-particles

2.1. CE characterization of polymer particles

Much of the initial work on the CE of colloidal polymer solutions was performed on polystyrene particles. Jones and Ballou evaluated different experimental conditions for the separation of numerous carboxylated and sulfated polystyrene particles of various size and charge [23]. More specifically, they focused on the effect that experimental parameters had on the efficiency, resolution, and mobility differences. It was found that much cleaner electropherograms resulted when using a very high pH (10.71) running buffer. The number of theoretical plates also generally increased at higher pHs (Fig. 1); however, this was not the case for the mobility differences or the resolution. They exhibited similar patterns of an initial rise in number of theoretical plates, then a sharp fall near pH 8.5, and finally, a slight increase at pH 11 [23]. The peaks were poorly shaped at low pHs though, and it was stated that a significant amount of error in the calculations of theoretical plates and resolution may have resulted from this. Voltage experiments were done at the optimal pH (10.71) and showed that the mobility difference of the particles became larger at higher electric fields. There was also an observed shift of each particle's mobility towards more negative values at higher applied voltages. A possible explanation offered was that the viscosity of the buffer decreased as a result of Joule heating. Another theory, not experimentally tested, was that shearing of the ionic atmosphere around the particles may have occurred at high electric fields, thereby uncovering more of the negatively functionalized surface. The resolution of the particles increased at higher electric fields, while the efficiency differed significantly for each particle.

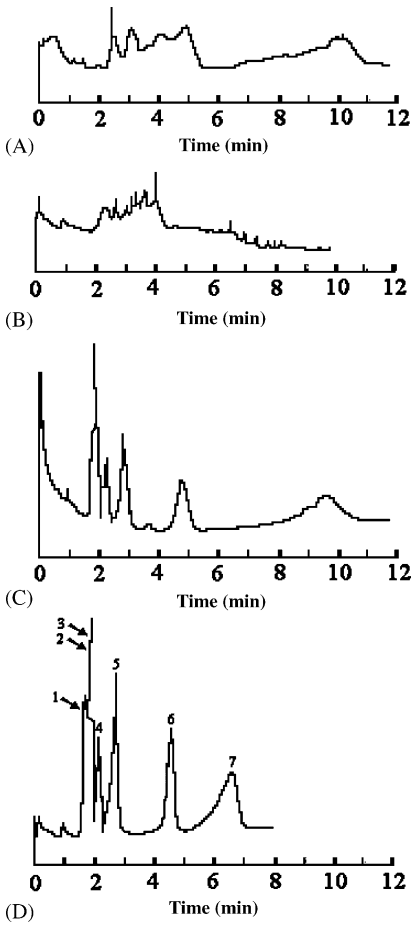

Fig. 1. Electropherograms of seven-component latex mixture at four pH values: (A) 6.64, (B) 7.21, (C) 8.49, and (D) 10.71. Peaks 1–7 correspond to particles of 0.030, 0.079, 0.070, 0.100, 0.200, 0.500, and 1.16 μm diameter, respectively. Capillary: 55 cm length, 75 μm i.d., 40 cm to detector, 30 kV. Phosphate buffer adjusted with appropriate amounts of NaOH. Reproduced from [23] with permission.

In a subsequent publication, it was shown that resolution and efficiency were in fact independent of the electric field, contrary to what was seen previously [24]. Upon careful consideration of all sources of band broadening in CE, it was concluded that the main contributions were from the finite injection zone length and the electrophoretic heterogeneity of the particles. Since these factors are independent of the electric field, the efficiency and resolution should be as well. After plots of current versus electric field were constructed, it was clearly evident from the deviation in linearity (when using a non-temperature regulated capillary) that a significant amount of heating was occurring inside the capillary. Similar plots using a thermostated CE device exhibited only slight deviations. The assumption that Joule heating

was responsible for the increase in mobility of the particles and that this in turn affected efficiency and resolution was correct, as indicated by the plots of mobility versus applied potential.

Work by Radko et al. focused on how well the CE of polymeric particles corresponded to electrokinetic theory [25]. After several experiments with various sized sulfated polystyrene particles at several ionic strengths, the conclusion was reached that the measured mobility was consistent with that predicted by the Oveerbeek–Booth electrokinetic theory. However, the presence of a "hairy layer" from extended polymer chains on the particle surface hindered a complete explanation. Electrophoretic heterogeneity was determined to be the most dominant factor contributing to band broadening in this case, but thermal effects from Joule heating also contributed (though a thermostated system was used), especially at high ionic strengths and electric fields.

Rosenzweig and Yeung were able to determine the presence of minute amounts of glucose-6-phosphate dehydrogenase (G6PDH) inside human erythrocytes (red blood cells) with a CE immunoassay method involving the use of antibody coated latex particles [26]. By measuring the change in light scattering of particles passing through a 20 μm capillary, the extent of agglutination of the particles could be ascertained; the aggregated (and thus larger) particles scattered the laser beam more than smaller single particles. Since the G6PDH induced agglutination of the particles and higher concentrations induced more agglutination, the amount of G6PDH could be indirectly determined by measuring the degree of light scattering. When the contents of a lysed erythrocyte were placed inside the capillary, the degree of light scattering (extent of agglutination) gave a direct indication of the amount of G6PDH present in a single human red blood cell.

Duffy et al. used a specialized CE instrument with laser-induced fluorescence detection (LIF) to identify single polymeric particles [27]. The electrophereograms exhibited sharp spikes corresponding to the individual particles. Significant differences were observed between the borate and borate–SDS running buffers in which the experiments were performed. SDS containing buffers produced faster migration times and a narrower range of times than did simple borate buffers (Fig. 2). Adsorption of SDS monomers to the particle surface was believed to be responsible for this effect. Since SDS is negatively charged, it tended to further enhance the negative charge on the particle and resulted in faster migration times in the reversed polarity mode. Two-dimensional plots could also be constructed using the LIF signal and the particle mobility; these plots provided an alternate tool for characterizing the particle size.

There have been a small number of publications in which the electrophoretic mobilities of colloidal polymer particles were determined by CE and then compared to the values obtained by laser Doppler velocimetry (LDV) measurements [28,30]. The electrophoretic mobility measurements were used to characterize the colloidal particles in terms of surface charge or size. This can be done since it is well-known that the mobility of a particle is strongly dependent on its charge-to-size ratio. The degree by which either parameter is experimentally altered (while holding the other constant) can be observed by the corresponding change in the mobility measurements. Fourest et al. initially published work comparing the electrophoretic mobilities obtained by the two methods (LDV & CE) for a number of colloidal substances such as: sulfated and carboxylated polystyrene particles (PSPs), as well as SiO_2, Al_2O_3, and TiO_2 particles [28]. The effects of buffer type, as well as the concentration of the colloids injected, on the measured mobilities were investigated. Their results showed that the mobility of the polystyrene particles (measured by LDV) was dependent on the concentration of supporting electrolyte, but more interestingly, on the nature of the supporting electrolyte as well. The smaller and less charged cations (Li and Na) of the supporting electrolyte produced much more negative mobilities. The anions of the electrolyte were not expected to have an effect on the measured mobility since the polystyrene particles (PSPs) are anionic in nature and for the most part cations are expected to be present in their diffuse layer. This was similar to the effect noticed by Tsukagoshi et al. for carboxylic acid and phenylboronic acid-modified polymer particles [29]. There was also an observed effect on the concentration of the PSPs on the measured mobilities. At higher concentrations, the mobility was much more negative and

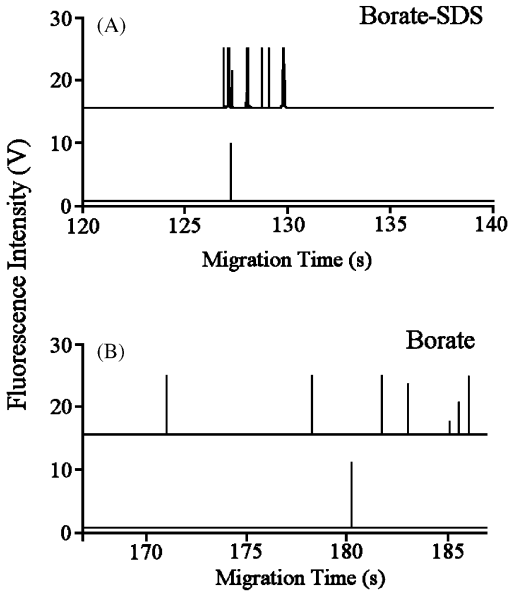

Fig. 2. Individual detection of microspheres. 6.0 μm diameter microspheres were diluted in either (A) borate–SDS buffer or (10 mM borate, 10 mM SDS, pH 9.3) and (B) borate buffer (10 mM borate, pH 9.3). The top trace in (A) and (B) corresponds to an electrokinetic injection (5 s at −100 V/cm) of several microspheres in a suspension. Similarly the bottom trace corresponds to the selective siphoning (1 s, −11.2 kPa) of one microsphere held on a slide by micropositioning the capillary injection on top of the microsphere. Separations were carried out at −400 V/cm in a 50 μm i.d., 36.3 cm long poly-AAP coated capillary. Reproduced from [27] with permission.

a corresponding increase in solution conductivity was also observed. The effect was attributed to the dissociation of the functional groups on the surface of the PSPs and was not seen when a supporting electrolyte was present (LDV). The mobilities of the PSPs obtained by both CE and LDV were compared directly and shown to be similar, except for those particles possessing a very high mobility. These particles were thought to be very sensitive to the surrounding environment, having large fluctuations with only slight changes in buffer composition.

VanOrman Huff and McIntire also examined the electrophoretic mobilities of polystyrene particles by using CE and LDV methods [30]. The mobilities of the particles were again found to be very similar for the two techniques, except when the particles possessed a positive charge. The large discrepancy between the two methods for amine latex particles was attributed to the possibility of interaction between the positive particles and the negatively charged surface of the capillary used for CE. The effect of surfactant adsorbed to the surface of the particles also was studied. The absolute magnitude of the electrophoretic mobility of sulfated polystyrene particles decreased as higher concentrations of a neutral polymeric surfactant were added to the run buffer. The observation was explained by a decrease in zeta potential (ζ: zeta potential, which is proportional to electrophoretic mobility) which declined to a limiting value as surfactant was added and the particle surface became saturated. The authors stressed that systems such as this are only useful under certain conditions. First, the analyte must not interact with the capillary walls, or else the decrease in mobility cannot be attributed solely to adsorption of surfactant to the surface of the particle. Any surfactant adsorbed to the capillary wall would lessen the interaction and cause a corresponding change in electrophoretic mobility. The analyte must be detectable, and lastly, the solution of analyte must be stable over time.

Hlatshawayo and Silebi also performed experiments on negatively charged PSPs with added SDS [31]. Several anionic PSPs were separated and identified using their specific experimental conditions. The detergent CHAPS (3-[(3-cholamidopropyl)dimethylammonio]propanesulfonic acid) was used to a limited extent by Radko et al. However, this study was more concerned with the upper size limits of molecular sieving by a polymeric network than in characterization of the polymeric particles [32]. Thus, far there has been only a single attempt to separate unmodified PSPs of various sizes [33]. The separations observed were thought to be due to ion adsorption from the run buffer and the acidic residues remaining on the particles from the polymerization process. Differences in the optical spectra of the particles helped in the identification of the peaks in the electropherogram. Experiments at several different pHs and voltages yielded only minimal changes in efficiency and mobility, but there appeared to be a definite relation between particle size and electrophoretic mobility [33].

There have also been CE experiments on other colloidal polymer particles, such as the work published by Janca et al. on the CE of polyaniline (PANI) particles [34]. When polyaniline is formed in the presence of certain stabilizers (i.e. poly(*N*-vinylpyrrolidone) or poly(vinyl alcohol)), analysis and characterization of the resulting polymer particles is easily performed. However, it is much more difficult when the particles are formed in the presence of colloidal silica, since simple separation methods such as centrifugation can no longer be applied. (The silica is similar in size to the polymer particles.) These experiments were an attempt to examine the feasibility of using CE to analyze the chemical uniformity of polyaniline particles formed in the presence of colloidal silica. Investigation of the influence of both pH and ionic strength on zeta potential indicated the possibility of separating polyaniline (PANI) and polypyrrole (PPy) particles from colloidal silica (Percoll) in the pH range of 4–11, provided the ionic strength was not too high [34]. However, when the individual mobilities of all three (PANI, PPy, and Percoll) were measured, and the reciprocal values plotted versus the zeta potential, it was seen that PPy particles could not be easily separated from the colloidal silica, but PANI particles could. A mixture of PANI and Percoll was subjected to CE and a slight separation was obtained. However, it was noted that the PANI peak shifted towards the Percoll peak when a mixture of the two was analyzed, compared to what was found when the particles were analyzed individually (Fig. 3). The authors speculate that this may be due to the formation of aggregates in the mixture [34].

The separation and characterization of a series of acrylic styrene copolymer particles was performed by Vanhoenacker

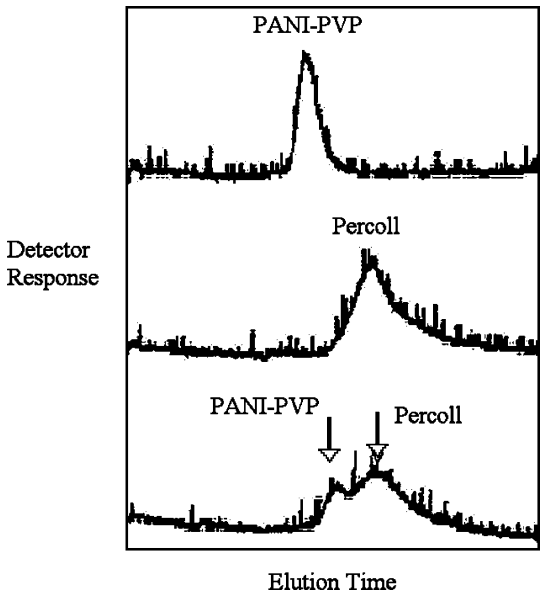

Fig. 3. Electrophereograms of the individual PANI–PVP and silica–PVP composite particles and of the separated mixture of both detected at a wavelength of 330 nm. Capillary: 75 cm length, 75 μm i.d., 20 kV, 0.02 M sodium tetraborate run buffer, pH ∼ 9.5. Reproduced from [34] with permission.

Table 1
Characteristics and mobility data of particles

Chemical composition	Particle diameter (nm)	Amount acid (%)	Zeta potential (mV)	Electrophoretic mobility (S.D.), (10^{-4} cm^2/V s)
2-EHA/AA	65	5	−54	−5.03 (0.03)
2-EHA/MAA	68	5	−56	−5.48 (0.05)
2-EHA	69	0	−59	−5.75 (0.05)
2-EHA/MAA	50	3	−59	−5.94 (0.06)
2-EHA/MAA	270	3	−66	−7.13 (0.05)

Experiments carried out in a 75 μm × 67 cm (58.5 cm effective length) capillary, buffer consisted of 5 mM NaH_2PO_4 adjusted to pH 9 with NH_3, 30 kV. Reproduced with permission [35].

et al. [35]. Particles of roughly the same size but varying compositions (different percentage of acrylic monomers) were analyzed to determine the effect of surface chemistry on separation. The opposite experiments were also performed (i.e. same chemical composition, but different size particles) to determine the effect of size on separation. The particles of differing chemical composition gave a separation but, as is mostly the case for these types of particles, displayed poor efficiency. In this case, the measured zeta potentials for each particle showed variation (a logical conclusion given the differing compositions) and allowed for a separation to be obtained. Slightly more complex behavior was displayed by the particles which varied in size but not chemical composition. The largest particles, having the most negative zeta potential, were detected last. The trend followed for smaller particles; those possessing less negative zeta potentials were detected before those that had more negative potentials. There was not, however, a linear relationship between the increase in electrophoretic mobility and the increase in zeta potential (both negative in value) (Table 1). This observed deviation was attributed to the relaxation effect, which differs for particles of different sizes. Mixtures of acrylic and urethane particles were also analyzed but aggregation caused difficulties in separation [35].

One factor relevant to all studies on colloidal particles has always been debated. That is, whether or not the separation mechanism is electrophoretic in nature or based on some other mechanism (i.e. size or particle–wall interactions). The earliest results indicated that separation was based on particle–wall interactions, since a strong dependence on size to separation was observed regardless of the charge/mass ratio. It should be pointed out that the capillaries used in this study were treated with a cationic surfactant (cetyltrimethylammonium bromide), which may have affected the results [36]. Currently, it appears that electrophoretic mobility dominates as the separation mechanism since excellent relationships are observed between charge/size ratios and migration times [33,34,39]. The observed independence of electric field on band broadening observed by some researchers reinforces this notion, by indicating a lack of particle–wall interaction [24]. The measurements of the mobility of polymeric particles by LDV, as well as the good agreement of those measurements to those obtained by CE establish the consensus that is presently held: that the separation of polymeric particles is mainly electrophoretic in nature.

2.2. Inorganic particles

The first attempt at a separation of inorganic colloidal species was done in 1991 by McCormick for silica sols [37]. A separation was obtained for a series of silica particles ranging in size from 5 to 500 nm. The standard buffer was a 5 mM ammonium hydroxide and 9.3 mM ammonium chloride solution. This buffer permitted a partial separation of several of the particles in a relatively short time (<20 min). Higher concentrations (2× standard) resulted in much better resolution of the smaller particles, but prohibitively long migration times for larger particles also resulted. These results are not unexpected since the increase in ionic strength not only slows the electroosmotic flow, but also causes a compaction of the diffuse layer, akin to what was found for polymeric particles (see previous section of the review). Similar experiments were performed on derivatized silica particles to examine their potential usefulness in CEC; however, the micro electrophoresis format was utilized [38].

Some similarities exist between polymeric & inorganic particles. Among those found by Fourest et al. were: (i) measured mobilities (by LDV) exhibited a dependence on the ionic strength; when the ionic strength increased, the mobility decreased, similar to PSPs; (ii) the colloidal oxides showed a change in mobility (as measured by LDV) when the concentration injected changed. Difficulty arose in the analysis of colloidal oxide particles by CE though, since they aggregated to a large extent in some buffers but not in others (this is one of the main differences between the colloidal mineral oxides and polymeric particles). Due to this problem, results for LDV of oxide particles were not compared to those for CE. It was concluded that CE is best used as a complimentary method to LDV for the characterization of colloidal particles. While CE is advantageous for separations, analysis is not possible without altering the natural environment of the colloid (a compatible run buffer must be used). In the same sense, LDV is capable of obtaining mobility data on unaltered samples, but problems occur if more than one colloid is present. Later publications by this group showed the complementary nature of the two techniques [39]. When mixtures of particles were prepared and subjected to analysis, as opposed to the single entities, these shortcomings and advantages became apparent.

Some degree of similarity in the CE behavior of polymeric and mineral oxide particles was also observed by

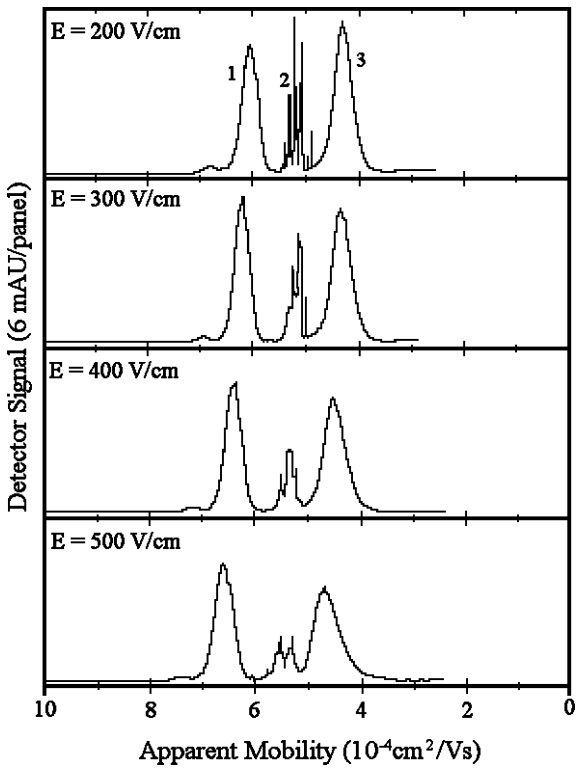

Fig. 4. Capillary zone electrophoretic separations at four electric field strengths of a mixture containing 0.015% (v/v) each of γα-Al_2O_3 (1), Fe_3O_4 (2), and TiO_2 (3) particles in 5.00 mM carbonate buffer, pH 10.6. The *x*-axis has been converted from units of migration time to apparent mobility. Capillary effective length: 30.3 cm, total length: 37.0 cm, 96 μm i.d. Reproduced from [40] with permission.

Ballou and Petersen [40]. The separation and characterization of Al_2O_3, TiO_3, Fe_2O_3, Fe_3O_4, and UO_2 particles had been performed previously [41,42]. In this instance, the same particles were analyzed under two different high pH systems, in order to optimize results. CZE results of γα-Al_2O_3, Fe_3O_4, and TiO_2 in 5.00 mM carbonate buffer, pH 10.6, show a good separation of the three particles. At low electric fields (below 300 V/cm) (Fig. 4) the selectivities and efficiencies appeared to be independent of electric field. This was in good agreement with results obtained for PSPs in a thermostated system [24]. However, at high electric fields the efficiencies dropped significantly (41%). The efficiencies of PSPs also displayed changes at higher electric fields in a non-thermostated system. The changes in both cases (mineral oxides and non-thermostated PSPs) were attributed to deviations from an Ohm's law plot, which gives an indication of significant Joule heating inside the capillary. However, the efficiency of mineral oxide peaks was observed to decrease, while the opposite was true for PSPs. Aside from these findings; the focus of the study was the optimization of the separation of the particles in two different buffer systems: carbonate and pyrophosphate. At high buffer concentrations, selectivities were enhanced, while efficiency decreased for both systems. The results also showed excellent run-to-run reproducibility. The R.S.D. for the migration time of a UO_2 standard was 0.092% for triplicate runs.

Ferrofluids have also been characterized using CE [43]. Ferrofluids are simply magnetic particles stabilized in non-magnetic carrier fluids. Similar to polyaniline particles, these substances acquire their charge from the stabilizers that are present during their formation. A series of cationic and anionic ferrofluids were analyzed by standard techniques of varying the pH, ionic strength and voltage. Minimal changes were observed in the measured electrophoretic mobility of all particles when the pH was varied over the range of 5–12. There was, however, a significant decrease in the measured mobility of a cationic ferrofluid in the pH range of 2–4. The investigators stated that better resolution was obtained between the ferrofluid particles and impurities present when lower voltages were used (15 kV versus 30 kV). There is, however, no mention of the effect of voltage on the measured mobility that is sometimes observed in these systems (i.e. particulate). A comparison of the values of electrophoretic mobilities obtained by micro- and capillary electrophoresis revealed that the CE values were lower in every instance. However, the reasons for this were not discussed.

The surface charge on gold nanoparticles arises from strongly adsorbed citrate ions and not from artificial modification or pH dependent functionalities, as is the case for polymeric and mineral oxide particles. Since gold particles possess a surface charge, they are able to be analyzed by CE just as are other charged colloidal/nano particles. Schnabel et al. were among the first to subject such gold particles to analysis by CE [44]. The aim of their study was to characterize the gold nanoparticles by size. The separation of these particles was less important since mixtures of these are rarely found under normal circumstances. There was an observed inverse relationship between particle diameter and electrophoretic mobility; however, it was only evident at high ionic strengths ($I = 0.006$ mol/l) (Fig. 5). Use of too high of an ionic strength caused difficulty in the analysis

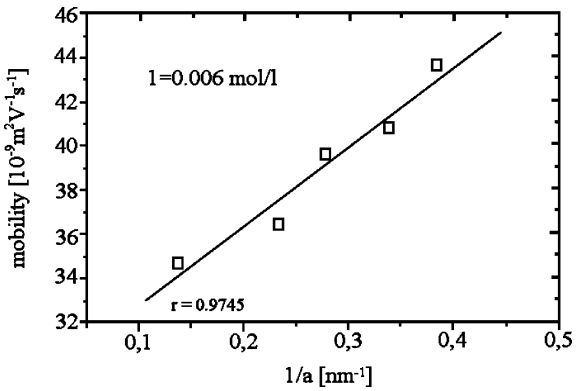

Fig. 5. Dependence of the electrophoretic mobility of the Au nanoparticles at given ionic strength on their core diameter. Capillary i.d.: 75 μm, total length: 35.0 cm, effective length: 27.0 cm. Ionic strength: 0.006 mol/l (acetic acid/Na acetate, pH 5). Reproduced from [44] with permission.

because compaction of the diffuse layer surrounding the particles occurred and lead to a corresponding flocculation of the particles.

Templeton et al. utilized CE to probe the dispersity of functionalization on tiopronin MPCs (monolayer protected gold clusters) [45]. Reactions were carried out to both displace tiopronin from the surface of the MPCs and to attach additional groups upon the tiopronin itself. Since methods to characterize the dispersity of such particles are not prevalent, a new technique utilizing CE was attempted. Samples of the tiopronin MPCs and *N*-(methyl)-*N*′-(ethylamine)-viologen dinitrate ($MEAV^{2+}(NO_3^-)_2$) modified MPCs were analyzed at a pH of 9.3. The negatively charged surface of the tiopronin MPCs yielded a series of wide overlapping peaks appearing at a migration time of 12–20 min (the EOF appeared at 3.7 min). On the other hand, the positively charged MEAV groups resulted in a sharp peak appearing at ∼2.0 min. Calculations using the mobility data indicated that the effective charge on the tiopronin MPCs was −7.4, and that of the MEAV MPCs to be +8.1. These values were both significantly different from the number of functional groups estimated on the surface, but not unexpected, since the effective charge is also the result of the screening that may occur from the ionic atmosphere formed around the particle by the surrounding buffer [45].

2.3. Viruses, bacteria, and fungi

Early work in microbial analysis by CE was performed in 1987 by Hjerten et al. who demonstrated that Tobacco mosaic virus (TMV) and *Lactobacillius casei* were transported similarly close to the EOF [46]. Electropherograms for each were obtained using a 100 μm i.d. capillary (coated with methylcellulose or linear polyacrylamide) and an appropriate Tris buffer. The TMV virus was studied again later by Grossman and Soane who determined that the orientation of the virus had an effect on its electrophoretic mobility [47]. Since the virus is oblong in shape, different orientations resulted in more or less frictional drag from the surrounding fluid. Higher electric fields aligned the virus more with the direction of the electroosmotic flow and created less frictional drag. An increase of more than 6% in the measured electrophoretic mobility was observed over the range of the electric fields studied.

Kenndler and co-workers exhaustively studied the human rhinovirus (HRV) in a number of publications. The first was a study to determine the isoelectric point (pI) of the human rhinovirus [48]. This was followed by a CE study showing that the HRV peaks could be reproducibly identified [49]. When HRV was analyzed using CE, a large peak consistently appeared at 3.6 min (see Fig. 6). A series of experiments then ensued to unequivocally assign the peak to the human rhinovirus. First, the virus was heated to denature it. The denaturing not only resulted in the loss of RNA from the viral capsid, but also various other structural changes. After the heated sample was subjected to CE, the main peak disappeared and a new peak at ∼4.8 min appeared, presumably from the released RNA. In order to determine whether or not this peak was in fact RNA, the virus was treated with RNase both before and after heating. Results showed that the major peak at 3.6 min was unaffected by treatment with only RNase; however, when the virus was heated first and then treated with RNase, the peak at 4.8 min disappeared. Several small peaks also appeared, most likely from the degradation of the RNA peak by RNase. The use of monoclonal antibodies also helped the absolute identification of the peak at 3.4 min as HRV. These antibodies caused aggregation of the HRV and when the sample was centrifuged, a decrease in the peak identified as HRV was observed. It is worth noting that small amounts of SDS, deoxycholate,

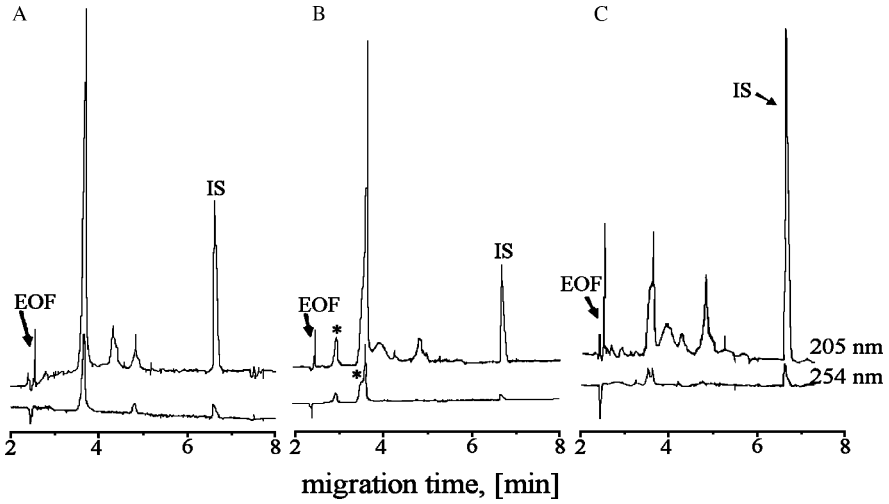

Fig. 6. CE separation of three different batches of purified HRV2. Virus recovered from cell supernant (A); virus recovered from cell pellet, lower fraction of sucrose gradient (B); and higher fraction of the sucrose gradient (C). Peaks marked with asterisks were present only in sample B. Virus concentration, ∼0.25 mg/ml in 1:10 diluted BGE without SDS added. Capillary, 50 μm i.d. × 50.0 cm, uncoated; effective length 41.5 cm. Buffer, 100 mmol/l borate, pH 8.3, containing 10 mmol/l SDS. Voltage, 25 kV. IS, *o*-phthalic acid 20 μg/ml. Reproduced from [49] with permission.

Triton X-100-R or some combination of the these surfactants were added to the run buffer for all of the experiments reported by this group. This was done to prevent adsorption of the virus to the capillary wall. In later work, the identification of other products that resulted from denaturing of the virus, namely, the 80S and 135S structural units, was attempted [50]. By using specific monoclonal antibodies (in one instance an antibody that binds exclusively to only subviral particles) the 80S particles could be centrifuged out of solution. After subsequent analysis of the supernant by CE, there was a decrease in the peak tentatively labeled as 80S, while the native virus peak was unaffected. The identification of the 135S particles was not successful.

A number of different serotypes of the human rhinovirus were also studied by Okun et al. [51]. The previous characterization by CE of the HRV2 serotype provided significant proof that peaks obtained indeed belonged to HRV, but in this case a post column infectivity assay was employed to aid in the identification of three more HRV serotypes: HRV14, HRV16, and HRV49. After the appropriate conditions were found, (i.e. pH and type of detergent) the different serotypes exhibited different electrophoretic mobilities. They varied from 9.6×10^{-9} to 22.7×10^{-9} m^2/V s. Fractions were then collected from the capillary and healthy HeLa cells were incubated with each fraction. Those fractions which corresponded to the eluting HRV2 and HRV14 cells showed the highest rates of infectivity (as determined by cell lysis), thus confirming the existence of infectious viral particles.

Affinity capillary electrophoresis (ACE) is a relatively new technique, but has provided a great deal of information concerning the interaction of a wide variety of molecules and macromolecules. For a comprehensive review of these methods, see [52]. ACE was used by Okun et al. to determine the extent of interaction between HRV and certain monoclonal antibodies [53]. A continual shift in the initial peak belonging to the native retrovirus was observed upon incubation with increasing amounts mAb 8F5, until an excess of mAb 8F5 was added, which caused a peak for free mAb 8F5 to appear. Similar observations were made with HRV14 and mAb 17-IA confirming complex formation. These experiments were extended to determine the stoichiometry between the monoclonal antibodies and HRVs [54]. The mAb to HRV ratio was determined for two cases: high affinity and intermediate affinity systems. For the high affinity system, a constant amount of mAb 3B10 was incubated with increasing amounts of HRV2. The aggregated viruses were centrifuged and the remaining mAbs were analyzed by CE. By plotting the peak area of mAb obtained by CE analysis versus the amount of HRV2 added, a linear binding curve was constructed. The *x*-intercept of such a curve can be used to determine the stoichiometry between the two analytes. For this case, a ratio of 1:18 HRV to mAb was obtained. For the intermediate system, a constant amount of mAb 8F5 was incubated with varying amounts of HRV2. In this case a peak for both the free mAb 8F5 and the complex were observed (the sample was not centrifuged), but as more HRV2 was added, a decrease in the free mAb peak was clearly evident. This data was used to construct a similar binding curve, but since this was a case of intermediate binding, the curve was not linear and resulted in a slight underestimation of the stoichiometry. The obtained ratio was 1:28, but by considering the viral symmetry and the foreseen underestimation, the experimental ratio was determined to agree well with the expected number of 1:30. Comparable results were acquired by stoichiometric studies of HRV2 with VLDLs (very low density lipoprotein receptors) [55].

The only attempt at studying a virus other than the human rhinovirus was by Mann et al. on an adenovirus [56]. The experiments were carried out using PVA coated capillaries approximately 57 cm in length and a 25 mM sodium phosphate buffer. Use of non-coated capillaries resulted in blank electropherograms, presumably from viral adsorption to the capillary wall. The electrophereograms from successful experiments yielded a major peak at 9–10 min along with minor trailing peaks. The viral activity was measured for several collected fractions and found to be highest in the region of 7–10 min, where the main and minor viral peaks resided. Protein based estimates for the concentration of virus injected were 4.9×10^{10} particles/ml (STD $\pm$ 2.2×10^{10}). The pH and the ionic strength were optimized at 7 and 25 mM phosphate, respectively.

Bacteria can be as much as 10^2–10^3 times larger than viruses; the increasing size leads to increased complexity. Viruses are known to exist mainly in one of two forms: helical or icosahedral. While viral capsids are composed entirely of protein, they typically contain only a few types. By their very nature, viruses are highly symmetrical, uniform and simplistic. This is not the case for bacteria; they can adopt an enormous variety of shapes and sizes, both among and within species. The outer membranes also have a large number of lipids, proteins, and techoic acids. [57]. The wide variety of physiological differences makes characterization of bacteria by CE somewhat more difficult than viruses.

Ebersole and McCormick were among the first to successfully subject bacteria to analysis by capillary electrophoresis [58]. In their publication, broad single peaks were obtained for a series of four bacteria: *S. pyogenes* (peak co-migrates with another), *S. agalactiae*, *S. pneumoniae*, and *E. faecalis*, using 250 cm long, 100 μm i.d. capillaries (see Fig. 7). The bacteria tended to migrate close to the electroosmotic flow (EOF) front when short capillaries were used; these capillary dimensions (especially the length) allowed sufficient time for the bacteria to distance themselves from the EOF front and from each other. Artificial mixtures of the bacteria were separated and fractions were recovered with greater than 98% purity in most cases. Culturing of the collected fractions showed significant numbers of colonies with little or no contamination. This demonstrated the ability of the technique to allow cells to remain viable during analysis. Pfetsch and Welsch were able to separate *P. putida*, *Pseudomonas* sp. and *A. euthrophus* under similar conditions (250 μm i.d. 250 cm length capillaries) [59]. The electrophoretic bands

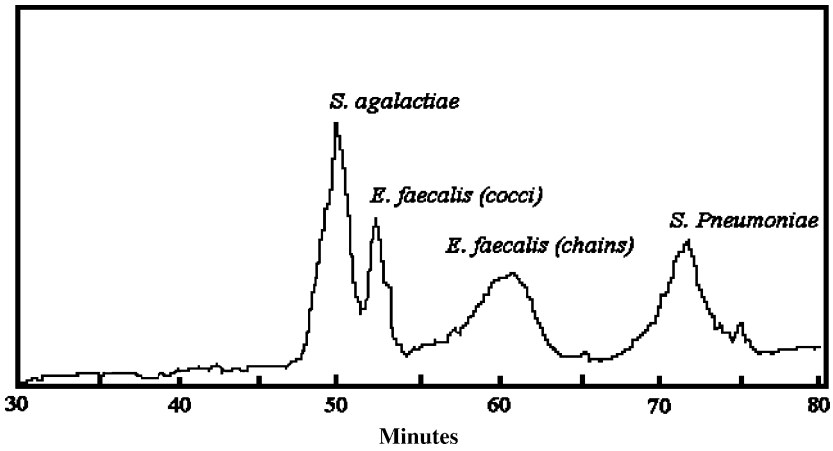

Fig. 7. CZE separation of a ternary mixture of *S. agalactiae*, *E. faecalis*, and *S. pneumoniae* bacteria. Reproduced from [58] with permission.

for the bacteria were considerably wider than those normally obtained for molecules, similar to [58], this was partially attributed to the variation in surface charge-to-size ratio and thermal field flow fractionation (TFFF) effects. Baygents et al. used CE to confirm results produced by MARK (microbe and radiolabel kinesis) studies on two types of bacteria (A1264 and CD1) obtained from sediments and river water [60]. Retention data from MARK studies displayed a best fit to a bimodal distribution. CE analysis, using a moderately long fused silica capillary (47–57 cm) and a 10^{-2} M MOPS buffer, confirmed the existence of two distinct bacterial populations having slightly different electrophoretic mobilities. A large collection of electrophoretic mobility data for several different bacteria was collected in [61]. Broad but reproducible peaks were apparent for each bacterial species using 50 μm i.d. capillaries 80 cm in length with a 10 mM phosphate buffer. Activity measurements were also reported in this publication by introducing a small amount of an exogenous electron acceptor (2,6-dichlorophenolindophenol, DCIP) along with an oxidizeable substrate (glucose) into the run buffer. A valley appeared in the electropherograms between the migration times of the bacteria (*Escherichia coli*) and the DCIP. This valley represented the region of reduced DCIP the *E. coli* produced using glucose as a substrate and also indicated that viable and active cells were being analyzed. Yamada et al. compared the separation of *C. cartae* and *A. tumifaciens* by CE to capillary gel electrophoresis (CGE) [62]. CGE outperformed CE in terms of peak purity; peaks for CGE were generally greater than 98% pure, while those for CE were only 90% pure. Due to the nature of CGE, however, the overall analysis time was much longer than for CE. Since the peak area of the bacteria correlated well with the number of cells injected, the cell population could accurately be monitored over the course of several days. (Accurate as determined by comparison with fluorescence in situ hybridization (FISH) techniques.) Using any of the aforementioned techniques, the CE separation of bacteria was only possible if there were sufficiently large differences in the electrophoretic mobilities. In addition, compared to CE of molecules, the peak capacity was small due to the small differences in migration times and the large peak widths [59]. Consequently, the CE separation of microorganisms and other cells was not widely pursued.

Recently, Armstrong and co-workers established a method that yielded separations of intact microorganisms with short analysis times and sharp peaks. These "apparent efficiencies" were attributed to the use of a very dilute (0.025% (w/w)) polymer additive (polyethyleneoxide). In one particular study, this method enabled the effective separation of *M. luteus*, *E. aerogenes*, *P. fluorescens*, and *S. cerevisiae* in less than 10 min, with a capillary having dimensions of 100 μm i.d. and 27 cm length (see Fig. 8) [63]. For the first time, capillary dimensions, migration times, peak resolutions, and "apparent efficiencies" were comparable to the best molecular separations. The exact mechanism for the resulting separations was not completely understood in the early reports [64–66]. However, it was clear that the size, shape and charge of the particles affected the separation. It was subsequently shown that aggregation played a significant role in obtaining single reproducible peaks [67]. Visible microscopy of cell solutions before injection into the capillary displayed a good correlation between the number of peaks in the resulting electropherogram and the extent of aggregation of the cells in the solution. There was a marked reduction in the number of peaks by brief sonication of the microbial samples just before injection. Experimental results showed that larger aggregates migrated through the capillary slower than single cells. Upon sonication, the aggregates were dissipated, allowing the single cells to migrate freely through the capillary. This uniform solution allowed a single peak to be obtained [65].

The technique was used for a number of applications including determination of cell viability, quantitation of bacteria, and identification of the bacteria responsible for urinary tract infections [64–66]. Quantitation of bacteria was accomplished by dissolving a varying number of dietary tablets containing bacteria in run buffer and relating the peak area obtained to concentration of cells injected [64]. The resulting

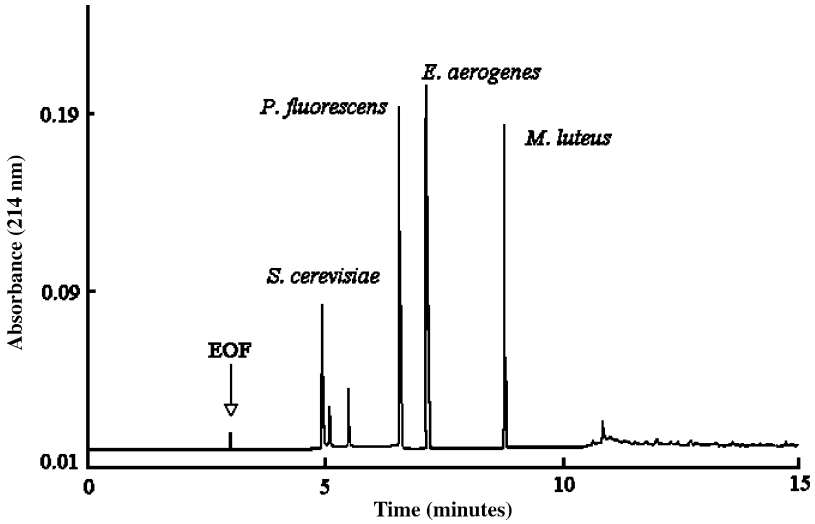

Fig. 8. Capillary electropherogram showing the separation of three bacteria and baker's yeast (*S. cerevisiae*) where small amounts of 600,000 M_W PEO are added to the running buffer. Note the relatively short migration times and the high efficiency. The arrow denotes the migration time of the EOF marker mesityl oxide. Conditions: 8:1 dilution of 4.5 mM TRIS, 4.5 mM boric acid and 0.1 mM EDTA in water with 0.5% PEO. Capillary: 100 μm × 27 cm (20 cm to detector), 10 kV. Reproduced from [63] with permission.

calibration curve yielded an R^2 value of 0.995 (cell counts compared to flow cytometry data). In conjunction with nucleic acid dyes, the calibration plots could be used to determine the number of viable cells in a given population. Analysis of *L. acidopholus* tablets utilizing this technique revealed that only 60% of the cells were viable. In further experiments the analytical figures of merit for determining cell viability by CE were determined [65]. A mixture of two bacteria and yeast were separated, identified, quantified, and the viability of each determined in a single run (Fig. 9) [65]. In a separate report, *S. saprophyticus* and *E. coli* (the two main causative agents of urinary tract infections) were identified in urine using a direct injection technique [66]. The major constituents of the urine matrix (e.g. urea and salts) migrated near the EOF while the bacteria migrated as a single sharp peak, several minutes later. *S. saprophyticus* generally had longer migration times than *E. coli*, allowing a differentiation between the two bacteria.

The use of a dilute polymer additive for CE bacterial analysis subsequently was used by other groups as well. Shintani et al. used a system consisting of sodium alginate polymer to obtain ultra high efficiencies for certain *Salmonella* strains [68]. Electrophoretic peaks for *S. enteritidis* were vastly improved when 0.01% sodium alginate was added to the run buffer and a similar, but smaller, effect was observed for *S. typhimurium*. A good correlation was found for injection cell number and the detection signal in relative fluorescence units ($R^2 = 0.9992$).

Several mechanistic aspects of the dilute polymer technique were studied using very specialized equipment [69–71]. By using a charge-coupled device (CCD) camera coupled with laser induced fluorescence, moving pictures of the capillary electrophoresis process could be taken (Fig. 10). The movies revealed that under certain conditions a band compaction process occurred inside the capillary as the bacteria traveled under the applied voltage (Fig. 11). This phenomenon appeared to be one of the reasons for the very narrow bandwidth of the peaks. Several factors and the influence each had on the compaction process were investigated [69]. Increasing the ionic strength of the buffer provided slightly more efficient and reproducible peaks, while increasing the pH served mainly to decrease electrophoretic heterogeneity and force the microbes toward the cathode. Different polymers were also considered and it was found that polyvinylpyrrolidone could also induce compaction, while polyacrylamide and poly (acrylamide-co-acrylic acid) could not. Different molecular weights of the polymers in the run buffer could be used to cause compaction to occur, but as higher molecular weights were used, longer migration times resulted. Wider injection plugs also produced longer migration times.

Several proposed pathways for the unusual compaction behavior were discussed in a recent publication [70]. The first proposed mechanism involved the presence of a "hairy" layer near the surface of the microbe from the dilute adsorbed polymer, not unlike the hairy layer proposed by Radko et al. for polymeric particles. The electrokinetic movement of small ions is slowed within this "hairy-layer" creating a localized region of lowered conductivity. If this results in a concurrent, significant local enhancement of the electric field, focusing can occur. This type of focusing is well-known for molecular analysis, but unlike molecular analysis, the sample here is not intentionally dissolved in a solution of lower ionic strength to create the effect. In addition, no other experimental focusing techniques such as pH gradients or sweeping were employed. A shape induced differential mobility model was also proposed. Some bacteria such as *E. coli* and *B. infantis* are rod shaped, similar to

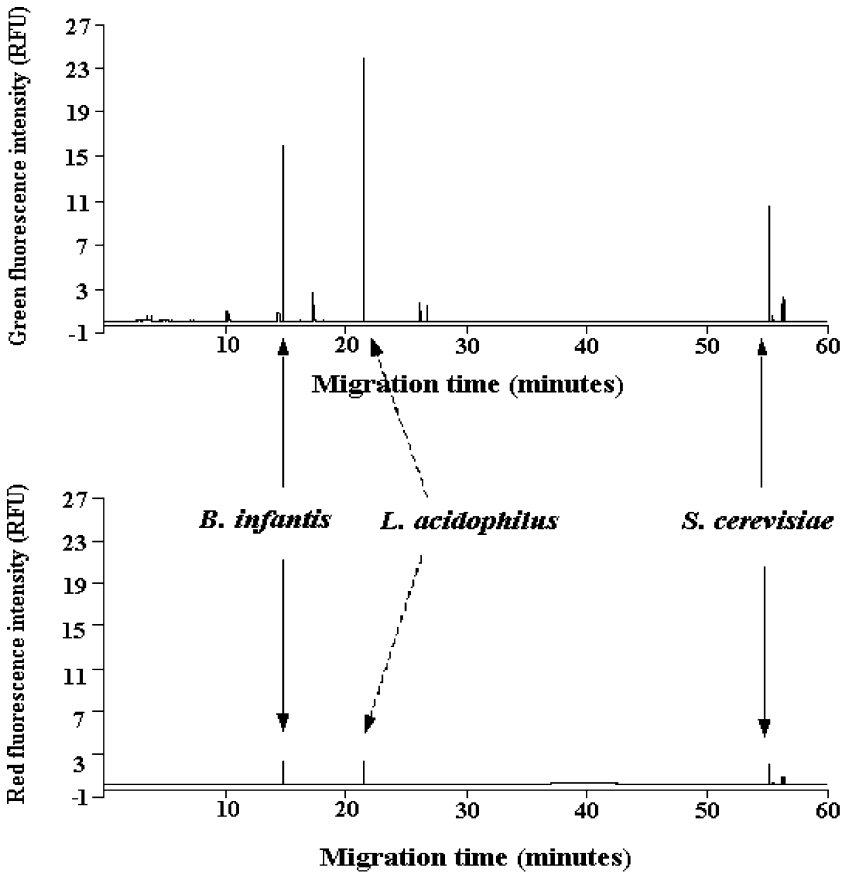

Fig. 9. Electropherograms showing the simultaneous separation of *B. infantis*, *L. acidophilus*, and *S. cerevisiae* and detection of (A) live (green fluorescence curve, top electropherogram) and (B) dead (red fluorescence curve, bottom electropherogram) cells. TBE buffer (w/0.025% PEO), capillary: 100 μm × 30 cm (20 cm effective length), 15 kV. Reproduced from [65] with permission.

TMV, and may exhibit varying mobilities based on their orientation in the capillary under an applied electric field. The differential mobilities may facilitate collisions between the bacteria and cause them to aggregate, as bacteria are known to do. It is believed that the polymer may serve a two-fold function in this process: to slow the EOF and allow sufficient time for the process to occur and to aid in particle–particle interactions. The last of the three proposed mechanisms was the "field-induced aggregation model". This model was based upon a recent theory which suggests that some colloidal particles (under certain specific circumstances) will form disc-like aggregates that align themselves perpendicularly to existing electric field lines [72]. Zheng and Yueng also investigated the mechanism underlying the compaction of bacteria in a polymer-based system [71]. Using a CCD camera coupled to a microscope, bacteria could be imaged at the single bacterium level. Visualization of the bacteria under the applied electric field showed that they moved at different speeds depending on their angular orientation with respect to the direction of flow, just as TMV do. Those at 0° (parallel to flow) moved fastest, while those at 90° (perpendicular to flow) moved slowest. The bacteria collided and agglomerated as they traveled, due to the varying velocities. The chances of another collision then increased due to the larger size of the newly formed aggregate. This "sticking" of the bacteria also contributed to the attainment of very narrow bandwidth of the CE peaks. It is important to note that the traditional term for efficiency does not apply to these types of systems. If the cohesive forces between the agglomerated bacteria are greater than the dispersive forces within the capillary, then there is no band broadening and the peak width is independent of migration time.

Use of coated capillaries has also yielded successful results in the analysis of bacteria and other microorganisms by CE. The coating serves to prevent adsorption of bacteria to the fused silica surface and to suppress the electroosmotic flow enough to allow the bacteria to travel mainly under the influence of their own electrophoretic mobility. *A. oxydans* was analyzed using a polyvinyl alcohol coated capillary and found to possess a positive charge since detection was possible only under normal polarity [73]. The electrophereograms contained groups of peaks and were attributed to both aggregation and heterogeneity of the bacteria. Similar to results obtained by other groups, the number of spurious peaks from aggregation was reduced after sonication [67]. In addition, the heterogeneity and distribution of peaks also changed depending on the growth phase of the bacteria. Buszewski et al. analyzed *P. fluorescens*, *E.*

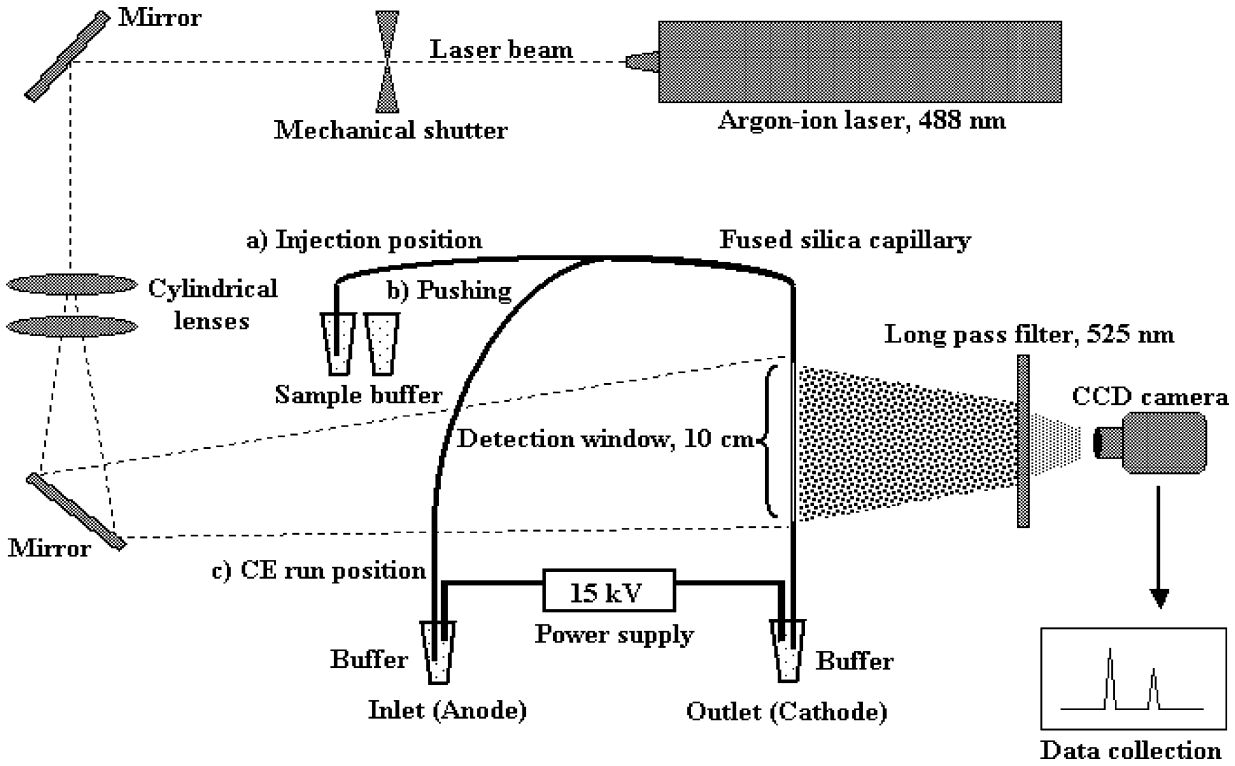

Fig. 10. CCD–LIF set-up. Reproduced from [69] with permission.

coli, *B. cereus* and *P. vulgaris* using acrylimide coated capillaries of extremely short length (8 cm effective). All peaks were detected in less than 7 min when reverse polarity was employed, however *P. fluorescens* and *E. coli* could not be resolved from each other (see Fig. 12) [74]. CIEF of yeast cells was accomplished by Shen et al. using a hydroxypropyl methylcellulose coated capillary [75]. The isoelectric points ranged from 5.2 for yeast cells in the early log phase of growth to 6.4 for cells in the stationary phase of the cell life cycle. An attractive feature of this method was that as little as five yeast cells could be detected in a single experiment.

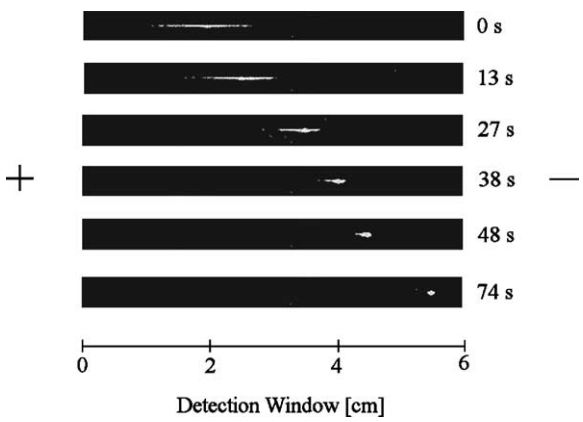

Fig. 11. Time resolved photographs showing the CE compaction of the injected sample zone and subsequent movement toward the cathode of *Bifidobacteria infantis*. At time = 0 s, the sample is the light zone between ~1.0 and 3.0 cm. Buffer: 0.0025% PEO (M_w = 600,000) in 3.94 mM TRIS/0.56 mM boric acid/0.013 mM EDTA, pH 9.1. Injection time: 2 s. Voltage: 7.5 kV. CE apparatus: homemade equipment with a 6 cm detection window. Reproduced from [70] with permission.

2.4. Mammalian cells, cell subunits and other biological particles

A majority of the work published on the analyses of mammalian cells was focused on red blood cells. Zhu and Chen analyzed a variety of RBCs (human, chicken, porcine and rabbit) using a wide bore (0.45 mm) fluorinated ethylene-propylene (FEP) capillary [76]. Addition of hydroxypropyl methylcellulose to the run buffer was crucial, without it single well-shaped peaks were not obtained. Surprisingly, the migration time of RBCs for each species varied significantly: chicken was detected at 28.3 min, porcine at 32.8 min, rabbit at 26.6 min and human at 14 min. When mixed samples were injected, the individual species did not interfere with each other and single peaks with consistent migration times were still obtained. However, a few factors degraded the experimental results. First, the FEP tubing broke down when subjected to high voltages and became useless after ~200 runs. Second, storage of the cells for extended periods of time affected the migration times [76].

Tsuda, et al. detected single red blood cells through a series of spikes which overlaid a broad peak spanning roughly 20 min [77]. The number of spikes resulting from absorbance detection at 430 nm correlated well with a method that involved use of a microscope and individual

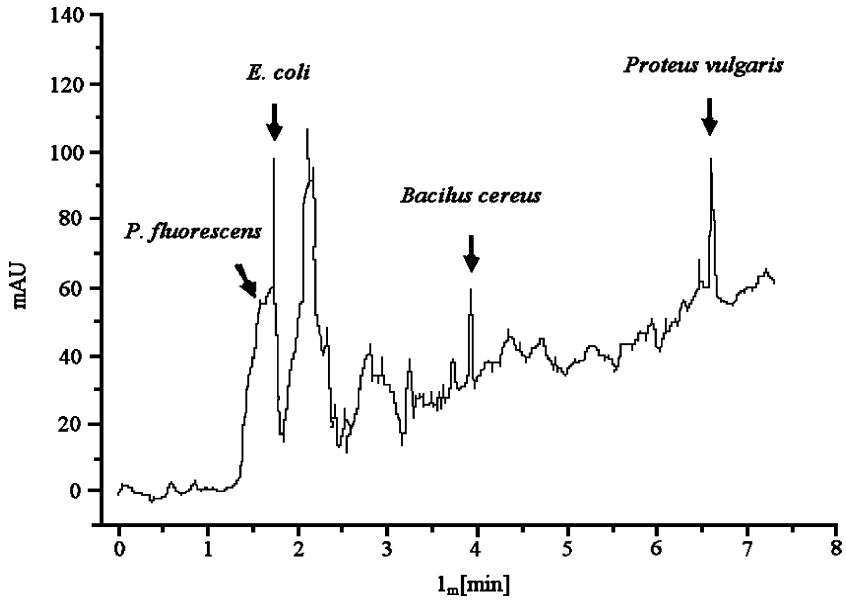

Fig. 12. Separation of four bacteria species on 8.5 cm distance using acrylamide modified capillary with suppressed EOF. Buffer: Tris pH 8.0, detection at 210 nm, $V = 20$ kV, injection 100 mbar s. Reproduced from [74] with permission.

counting of the RBCs, to construct an electropherogram. Using a more dilute injection of RBCs resulted in a much cleaner electropherogram, which allowed individual RBCs to be more easily distinguished from aggregates based on the peak height. Red blood cells have also been studied in micro-gravity [78]. Values for the electrophoretic mobility of RBCs were higher in micro-gravity than in normal gravity. It is believed that micro-gravity could have had a number of effects on the analysis of RBCs by CE. CCD images of the capillary revealed that the cells do not settle to the bottom of the capillary under reduced gravity; therefore, there is less interaction of the cells with the walls of the capillary. It is also believed that micro-gravity induces changes in the morphology of the cells and may reduce the viscosity of the run buffer, both of which could have resulted in the increased electrophoretic mobility [78].

Some of the simplest eukaryotic cells in nature are human RBCs which possess no nucleus or other specialized organelles. Indeed the pinnacle of cellular analysis by CE would then be the study of cells more complex than bacteria, yeast, viruses or RBCs. Recently, a method to differentiate between apoptotic rat cerebellar granule cells and normal cells utilizing CE was introduced by Gou et al. [79]. Two peaks were detected in the electropherogram resulting from an injection of granule neurons subjected to induced apoptosis, using a 100 μm i.d. capillary, 80 cm in length. When larger capillaries were used for electrophoresis, thermal band broadening caused an overlap of peaks, while use of smaller i.d. capillaries caused rupture of the cells. Optimization of pH and voltage resulted in two distinct and sharp peaks differing by 5 min in migration time. The procedure was tested against a staining method using methyl green pironin dye. An excellent correlation between the two methods for determining the percentage of apoptotic cells as a function of incubation time with the apoptosis inducing agent was observed. The authors mention the potential for this method in the diagnosis of Parkinson's disease [79].

He et al. demonstrated a method for the viability assessment of boar sperm [80]. Several factors that contributed to the reproducible attainment of both a single peak and a steady green to red fluorescent signal (for determination of live and dead cells, respectively) were outlined. Three factors had profound effects on the success of these experiments: (i) use of a semen extender for suspension of cells (cells placed in typical CE buffers are not stable and produced many peaks), (ii) appropriate ionic strength (varying the ionic strength had a dramatic effect on the green to red (G/R) fluorescence signals and increased the signal obtained for background contaminants) and (iii) use of a polymer additive (the addition of 0.01–0.05% PEO afforded both better peak shape and shorter analysis times). When a completely optimized system was used and a calibration curve constructed using the G/R signal (Figs. 13 and 14), the viability assessment of two samples was determined to be 37% and 82%, respectively (in agreement with flow cytometry measurements).

Arriaga and coworkers have analyzed intact intracellular structures (i.e. mitochondria and nuclei) utilizing CE [81–84]. Many assays exist for studying large collections of these species, however, these data represent an average for the entire organelle sample. Previously, there was no way to look at single organelles or variations within a group. CE-LIF though, along with a highly sensitive detector capable of rapid data acquisition, has allowed the detection and characterization of single organelles. This technique has been used to determine the amount of

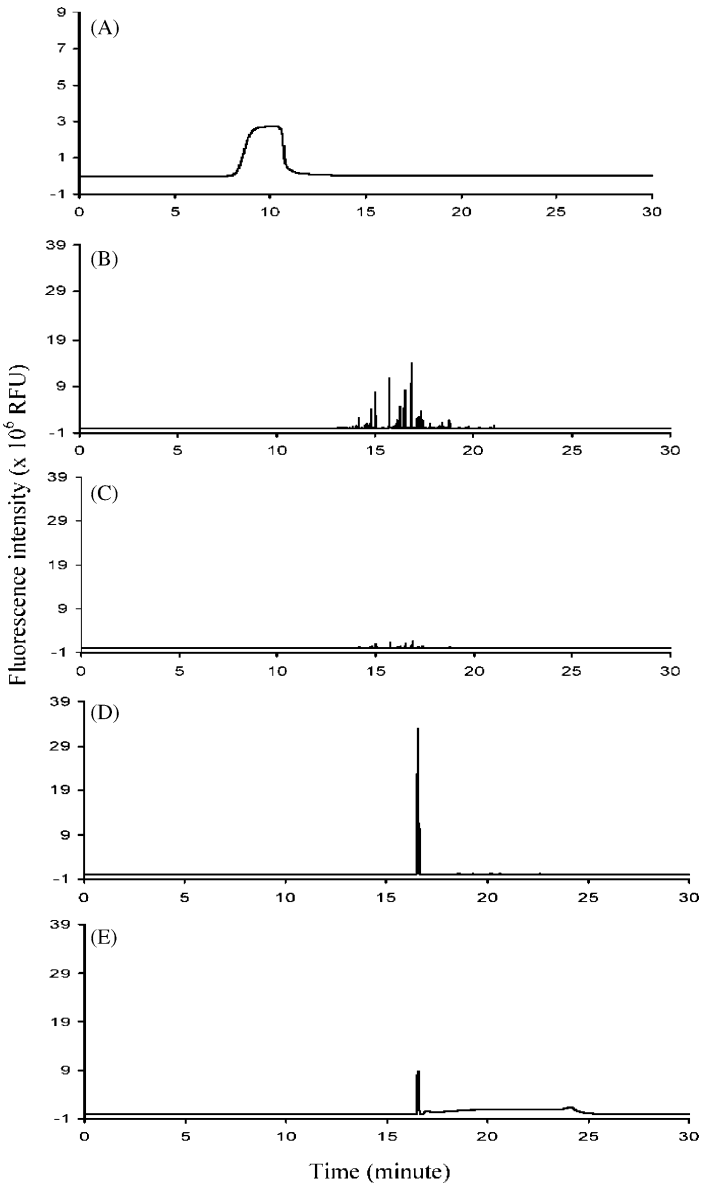

Fig. 13. Electrophereogram showing EOF marker peak (A) and boar sperm peaks (B)–(E). Generally, a cluster of peaks was observed if boar semen sample was washed and suspended in running buffer: (B) for green fluorescence signal and (C) for red fluorescence signal. A single sharp peak for sperm was easily obtained if boar semen was suspended in boar semen extender (X-CELL): (D) for the green fluorescence signal and (E) for red fluorescence signal. The running buffer consisted of 1 mM Tris, 0.33 mM citric acid, and 1% fructose with a pH of 6.9. All samples were injected for 10 s at 0.5 psi, and a 1.0 kV voltage was applied. Reproduced from [80] with permission.

cardiolipin (a phospholipid) in a mitochondrion (from NS1 cells) to be 2.2 amol (assuming 1000 mitochondria/cell) [81]. It has also been used to determine the average number of mitochondria per cell to be 52, and the distribution of protein per mitochondrion (for MAK mouse hybridoma cells) [82]. The electrophoretic mobility of single mitochondria was measured and found to fall within the range of -1.2×10^4 to -4.3×10^4 cm^2/V s for NS1 cells (Fig. 15) and -0.8×10^4 to -4.2×10^4 cm^2/V s for CHO cells [83]. Mobility measurements were also performed on the individual nuclei of NS1-mouse hybridoma cells in a similar manner [84].

Liposomes are spherical particles comprised of a lipid bilayer and an aqueous core. They form spontaneously when a dried film of lipids is agitated and/or sonicated in the presence of an aqueous solution. They are interesting in that they can be used as model systems for studies on biological membranes, as carriers in the cosmetic industry, and for drug delivery systems [85]. CE has been employed to a large extent to examine these particles and characterize them in terms of rigidity, permeability, surface charge, and stability [86–91]. The rigidity of liposomes was probed by altering the temperature of the capillary during electrophoresis [86]. It was assumed that if liposomes behave ideally, the migration time

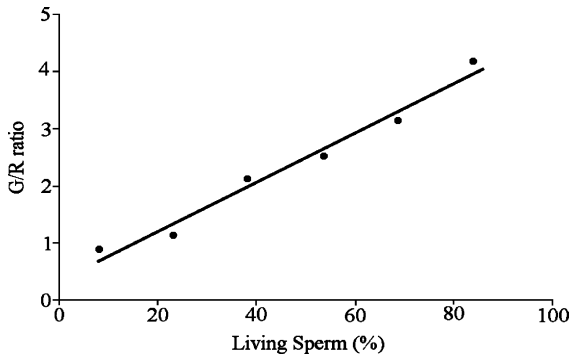

Fig. 14. Standard viability curve for boar sperm ($y = 0.043x + 0.3676$, $R^2 = 0.974$). Semen sample was diluted with BTS extender. Reproduced from [80] with permission.

would increase proportionally with the viscosity of the solution. Experimentally, however, a sharp discontinuity was observed in the plot of migration time versus viscosity. This could only be explained by a change in the hardness of the liposome; a soft liposome can distort in response to the increased friction caused by the increase in viscosity. This would, in turn, alter the expected migration time. A particle which remained rigid, such a latex bead, would not display such behavior and this was supported experimentally. Peak broadening from increased amounts of anionic lipids incorporated into the liposome structure was also attributed to a change in the rigidity of liposomes [87,88]. Studies utilizing CE have shown that slight changes in pH and buffer identity do not have a significant effect on the stability or permeability of liposomes [89,93]; however, elevated temperatures can cause contents to be released very quickly as the liposomes are destroyed. Standing for long periods of time and osmotic differentials cause a slow release of contents, however, there is no degradation of the liposomes themselves from this [90]. Extremes of pH though, along with high concentrations of organic solvents and detergents all cause deterioration of liposomal structure [89]. In addition to characterization by CE, liposomes have been used as an additive for electrokinetic capillary chromatography (ECC) [87,89]. In view of the success of a wide variety of other psuedophases and additives, this was not surprising. Probing of the strength of a complex between thermo/pH sensitive polymers and cationic nonphospholipid liposomes was also accomplished via CE [92].

Though many CE studies have revealed information about the surface characteristics and size of liposomes, liposomes have also been constructed with specific sizes and

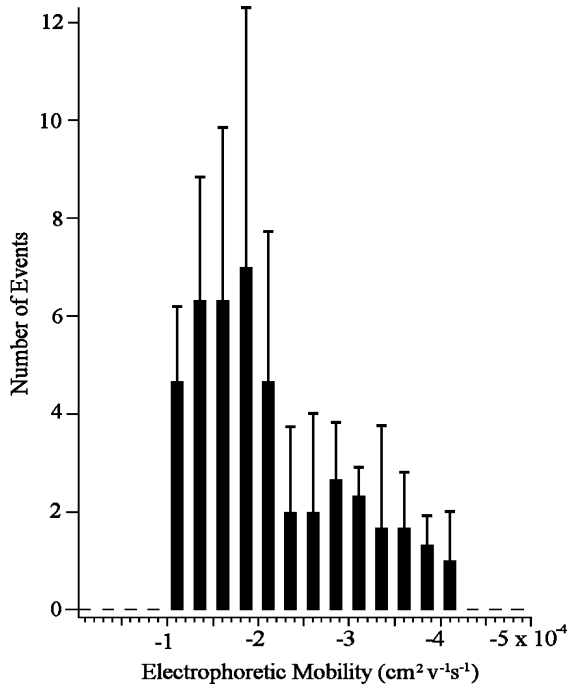

Fig. 15. Electrophoretic mobility distribution. The migration time for detected events with signals higher than 0.02 V were used to calculate the electrophoretic mobility of the event. Bins are 0.225×10^{-4} cm^2/V s wide. The mitochondrial isolate was analyzed in triplicate. The height of the thick bar represents the average; the thin line represents one standard deviation. Separations were performed at -200 V^{-1} in a 27.4 cm 50 μm i.d. poly-AAP coated capillary. 10 mM HEPES, 250 mM sucrose buffer. Reproduced from [83] with permission.

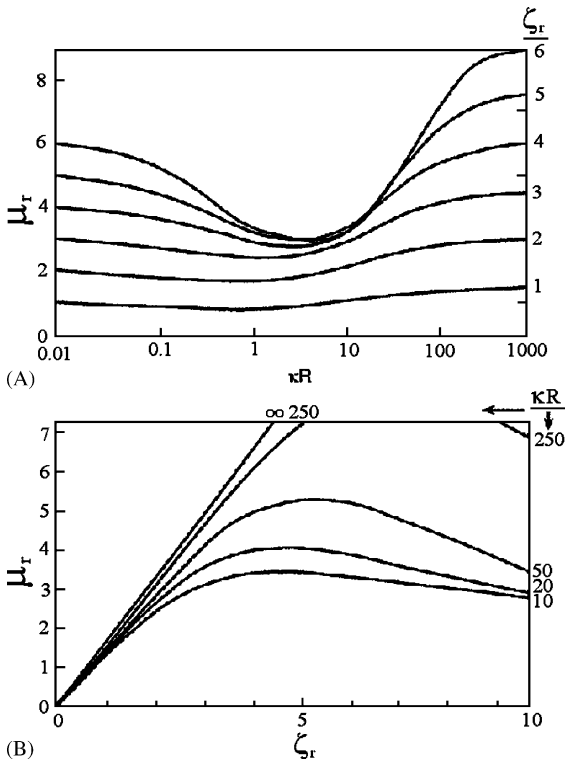

Fig. 16. Fig. 1A schematic representation of the dependencies of reduced (dimensionless) electrophoretic mobility, μ_r, of nonconducting spherical particles on the product of the reciprocal of the thickness of electric double layer, κ, and particle radius, R (panel A), and that on the reduced (dimensionless) ζ-potential of the particles, ζ_r (panel B). The curves are drawn on the basis of the results of Wiersema et al. [97] (panel A) and O'Brien and White [96] (panel B). Corresponding values of reduced ζ-potential (panel A) and of κR (panel B) are indicated near the curves outside the panel. Reproduced from [94] with permission.

surface qualities in order to obtain information about the fundamental reasons for their separation [94]. The electrical double layer surrounding a particle is known to influence its electrophoretic mobility. Generally, as the ionic strength of a solution increases the thickness of the double layer and the zeta potential both decrease. It is also true that for most cases, as the ionic strength of a solution is changed, the mobility is proportionately altered. However, there is a special case in which this trend is not obeyed; this case if referred to as the "relaxation effect". Because the ionic cloud surrounding a particle cannot establish itself instantaneously when it moves, the atmosphere is distorted. In front of the particle the atmosphere has not completely formed and the cloud behind it has not completely dissipated. This causes a displacement of the center of charge of the ionic atmosphere and a pull on the particle itself, since the atmosphere and the particle are opposite in charge [95]. This effect was found to be the fundamental factor governing the size dependent separation of liposomal structures [94]. The theoretical dependence of electrophoretic mobility on the κR factor (i.e. the reciprocal of the double layer thickness times the particle radius) and the zeta potential was found to exhibit unique behavior when the relaxation effect was taken into account (Fig. 16) [96]. The experimental results supported the theoretical prediction: that the electrophoretic mobility of a particle can become independent of and even decrease with increasing zeta potential at low ionic strengths, when the relaxation effect is present [94]. The measured mobility of a highly charged distearoylphosphatidylcholine–distearoylphosphatidylglycerol–cholesterol liposome at low ionic strength ($\kappa R \sim 10$) displayed such a decrease with increasing zeta potential (Fig. 17). Additionally, a set of two pairs of liposomes were constructed so that the size of the liposomes differed within each pair (by 68 nm in one case and 100 nm in the other). The liposomes were also tailored to have similar charge densities within each pair and to have different charge densities from one pair to the other (the pair with the smaller size difference was higher in surface charge density). When analyzed, the pair having the larger size disparity was not as effectively separated as the group which possessed the larger surface charge density. This behavior was said to directly point to a "relaxation effect"-governed separation mechanism.

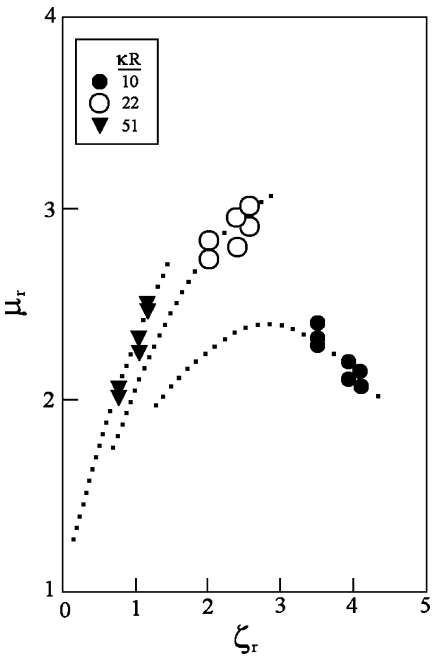

Fig. 17. Dependencies of reduced electrophoretic mobility of liposomes on reduced ζ-potential calculated on the basis of the surface charge density of the liposomes. Liposome preparations are L-179, -187, and -188. Tris–HCl buffer (pH 8) is of ionic strengths of 0.0011, 0.0054, and 0.0268. Reproduced from [94] with permission.

3. Concluding remarks

Capillary electrophoresis is becoming a valuable tool for the analysis of colloidal/nano particles because of its speed, simplicity, and separating capabilities. Many problems and difficulties that have been associated with the analysis of particles by CE, such as wall adsorption, aggregation, stability, poor efficiency, reproducibility, and electrophoretic heterogeneity have been circumvented by use of a variety of experimental approaches. These include use of wall coatings, use of dilute polymer additives, compatible buffers, pretreatments, and general care to find appropriate conditions suitable for analysis. The importance of colloidal/nano particles and the limitations of current methodologies have driven researchers to find newer, more effective CE approaches. Characterization of polymeric particles, inorganic particles, viruses, fungi, bacteria, red blood cells, and organelles has all been done utilizing CE. These experiments have provided an understanding of fundamental electrophoretic theory, the possibility of diagnosing a variety of diseases, and the ability to separate and identify viable cells. In order to become a widely useful and popular technique for the analysis of colloidal/nano particle systems additional work must be done. There needs to be a better theoretical understanding of these systems. Frequently the separation mechanism(s) and electrokinetic behavior are not well understood. Consequently optimization of each system is usually done by "trial and error". Also, the applicability of these techniques needs to be expanded. There is limited data on many colloidal systems, such as gold nano-particles, simply because of the perceived difficulties of using CE with these substances. There also needs to be a general improvement in the reproducibility of these methods. Of course, this is a factor that affects CE in general. As these issues are resolved, our understanding of these systems improves, and CE is extended to include other colloidal particles, the use and wealth of information obtained from the CE analysis of colloidal/nano particles will continue to grow.

References

[1] A.R. Timberaev, Electrophoresis 23 (2002) 3884.
[2] P.R. Haddad, P. Doble, M. Macka, J. Chromatogr. A 856 (1999) 145.
[3] P.E. Jackson, P.R. Haddad, Trends Anal. Chem. 12 (1993) 231.
[4] P.G. Righetti, Biopharmaceut. Drug Disposition 22 (2001) 337.
[5] V. Kasicka, Electrophoresis 20 (1999) 3084.
[6] P.G. Righetti, C. Gelfi, Capillary Electrophoreis Anal. Biotechnol. 1996, pp. 431–476, CRC Press, Boca Raton.
[7] N.K. Karamanos, Pharmakeutike 11 (1998) 56.
[8] S. Beale, Anal. Chem. 70 (1998) 279R.
[9] P.D. Grossman, J.C. Colburn, Capillary Electrophoresis, Theory and Practice, Academic Press, San Diego, CA, 1992. p. 113.
[10] P.D. Grossman, J.C. Colburn, Capillary Electrophoresis, Theory and Practice, Academic Press, San Diego, CA, 1992, p. 31–38.
[11] S.P. Radko, A. Chrambach, Electrophoresis 23 (2002) 1957.
[12] P.J. Wyatt, D.N. Villalpando, Langmuir 13 (1997) 3913.
[13] J.M. Singer, C.M. Plotz, Am. J. Med. 21 (1956) 888.
[14] L.B. Bangs, Pure Appl. Chem. 68 (1996) 1873.
[15] E.A. Medcalf, D.J. Newman, E.J. Gorman, C.P. Price, Clin. Chem. 36 (1990) 446.
[16] R. Elghanian, J.J. Storhoff, R.C. Mucic, R.L. Letsinger, C.A. Mirkin, Science 277 (1997) 1078.
[17] P.D. Rye, Bio/Technology 14 (1996) 155.
[18] S. Miltenyi, W. Muller, W. Weichel, A. Radbruch, Cytometry 11 (1990) 231.
[19] B.I. Haukanes, C. Kvam, Bio/Technology 11 (1993) 60.
[20] P. Hahn, et al., Radiology 175 (1990) 695.
[21] J.R. Phillipot, F. Schuber, Liposomes as Tools in Basic Research and Industry, CRC Press, Boca Raton, FL, 1995.
[22] H.S. Dearie, V. Spikmans, N.W. Smit, F. Moffatt, S.A. Wren, K.P.J. Evans, Chromatogr. A 929 (2001) 123.
[23] H.K. Jones, N.E. Ballou, Anal. Chem. 62 (1990) 2484.
[24] S.L. Petersen, N.E. Ballou, Anal. Chem. 64 (1992) 1676.
[25] S.P. Radko, M. Statsna, A. Chrambach, Electrophoresis 21 (2000) 3583.
[26] Z. Rosenzweig, E.S. Yeung, Anal. Chem. 66 (1994) 1771.
[27] C.F. Duffy, A.A. McEathron, E.A. Arriaga, Electrophoresis 23 (2002) 2040.
[28] B. Fourest, N. Hakem, R. Guillaumont, Radiochim. Acta 66–67 (1994) 173.
[29] K. Tsukagoshi, A. Yamaguchi, N. Morihara, R. Nakajima, M. Murata, M. Maeda, Chem. Lett. 9 (2001) 926.
[30] B. VanOrman Huff, G.L. McIntire, J. Microcol. Sep. 6 (1994) 591.
[31] A.B. Hlatshwayo, C.A. Silebi, Poly. Mater. Sci. Eng. 75 (1996) 55.
[32] S.P. Radko, M.M. Garner, G. Caiafa, A. Chrambach, Anal. Biochem. 223 (1994) 82.
[33] N.G. Vanifatova, B.Y. Spivakov, J. Mattusch, R. Wennrich, J. Chromatogr. A 898 (2000) 257.
[34] J. Janca, S. Le Hen, M. Spirkova, J. Stejskal, J. Microcol. Sep. 9 (1997) 303.
[35] G. Vanhoenacker, L. Goris, P. Sandra, Electrophoresis 22 (2001) 2490.
[36] B.B. VanOrman, G.L. McIntire, J. Microcol. Sep. 1 (1989) 289.
[37] R.M. McCormick, J. Liq. Chromatogr. 14 (1991) 939.
[38] O.L. Sanchez Munoz, E. Perez Hernandez, M. Lammerhofer, W. Linder, E. Kenddler, Electrophoresis 24 (2003) 390.
[39] B. Fourest, N. Hakem, J. Perrone, R. Guillaumont, J. Radioanal. Nucl. Chem. 208 (1996) 309.
[40] N.E. Ballou, S.L. Petersen, J. Chromatogr. A 834 (1999) 445.
[41] C. Quang, S.L. Petersen, G.R. Ducatte, N.E. Ballou, J. Cromatogr. A 732 (1996) 377.
[42] G.R. Ducatte, N.E. Ballou, C. Quang, S.L. Petersen, J. Microcol. Sep. 8 (1996) 403.
[43] A. Morneau, V. Pillai, S. Nigam, F.M. Winnik, R.F. Ziolo, Colloids Surf. 154 (1999) 295.
[44] U. Schnabel, C.H. Fischer, E. Kenndler, J. Microcol. Sep. 9 (1997) 529.
[45] A.C. Templeton, D.E. Cliffel, R.W. Murray, J. Am. Chem. Soc. 121 (1999) 7081.
[46] S. Hjerten, K. Elenbring, F. Kilar, J. Liao, A.J.C. Chen, C.J. Siebert, M. Zhu, J. Chromatogr. 403 (1987) 47.
[47] P.D. Grossman, D.S. Soane, Anal. Chem. 62 (1990) 1592.
[48] U. Scnabel, F. Groiss, D. Blaas, E. Kenndler, Anal. Chem. 68 (1996) 4300.
[49] V. Okun, B. Ronacher, D. Blaas, E. Kenndler, Anal. Chem. 71 (1999) 2028.
[50] V. Okun, D. Blaas, E. Kenndler, Anal. Chem. 71 (1999) 4480.
[51] V. Okun, B. Ronacher, D. Blaas, E. Kenndler, Anal. Chem. 72 (2000) 2553.
[52] R.M. Guijt-Van Duijn, J. Frank, G.W.K. Van Dedem, E. Baltussen, Electrophoresis 21 (2000) 3905.
[53] V. Okun, B. Ronacher, D. Blaas, E. Kenndler, Anal. Chem. 72 (2000) 4634.
[54] V.M. Okun, R. Moser, D. Blaas, E. Kenddler, Anal. Chem. 73 (2001) 3900.
[55] V.M. Okun, R. Moser, B. Ronacher, E. Kenddler, D. Blaas, J. Biol. Chem. 276 (2001) 1057.
[56] B. Mann, J.A. Traina, C. Soderblom, P.M. Murakami, E. Lehmberg, D. Lee, J. Irving, E. Nestaas, E.J. Pungor Jr., Chromatogr. A 895 (2000) 329.
[57] J.L. Ingraham, C.A. Ingraham, Introduction to Microbiology, 2000, Brooks/Cole, CA.
[58] R.C. Ebersole, R.M. McCormick, Bio/Tecnology 11 (1993) 1278.
[59] A. Pfetsch, T. Welsch, Fres. J. Anal. Chem. 359 (1997) 198.
[60] J.C. Baygents, J.R. Glynn Jr., O. Albinger, B.K. Biesemeyer, K.L. Ogden, R.G. Arnold, Environ. Sci. Technol. 32 (1998) 1596.
[61] M. Torimura, S. Ito, K. Kano, T. Ikeda, Y. Esaka, T. Ueda, J. Chromatogr. B 721 (1999) 31.
[62] K. Yamada, M. Torimura, S. Kurata, Y. Kamagata, T. Kanagawa, K. Kano, T. Ikeda, T. Yokomaku, R. Kurane, Electrophoresis 22 (2001) 3413.
[63] D.W. Armstrong, G. Schulte, J.M. Schneiderheinze, D.J. Westenberg, Anal. Chem. 71 (1999) 5465.
[64] D.W. Armstrong, J.M. Scneiderheinze, J.P. Kullman, L. He, FEMS Microbiol. Lett. 194 (2001) 33.
[65] D.W. Armstrong, L. He, Anal. Chem. 73 (2001) 4551.
[66] D.W. Armstrong, J.M. Scneiderheinze, Anal. Chem. 72 (2000) 4474.
[67] J.M. Scneiderheinze, D.W. Armstrong, G. Schulte, D.J. Westenberg, FEMS Microbiol. Lett. 189 (2000) 39.
[68] T. Shinitani, K. Yamada, M. Torimura, FEMS Mirobio. Lett. 210 (2002) 245.
[69] M. Girod, D.W. Armstrong, Electrophoresis 23 (2002) 2048.
[70] D.W. Armstrong, M. Girod, L. He, M.A. Rodriguez, W. Wei, J. Zheng, E.S. Yeung, Anal. Chem. 74 (2002) 5523.
[71] J. Zheng, E.S. Yeung, Anal. Chem. 75 (2003) 818.
[72] B. Khusid, A. Acrivos, Phys. Rev. E 54 (1996) 5428.
[73] N.Y. Tsibakhashvilli, N.V. Asatiani, M.K. Abuladze, B.G. Birkaya, N.A. Sapojnikova, L.M. Mosulishvili, H.N. Holman, Biomed. Chromatogr. 16 (2002) 327.
[74] B. Buszewski, M. Szumski, E. Klodzinska, H. Dahm, J. Sep. Sci. 26 (2003) 1045.
[75] Y. Shen, S.L. Berger, R. Smith, Anal. Chem. 72 (2000) 4603.
[76] A. Zhu, Y. Chen, J. Chromatogr. 470 (1989) 251.
[77] T. Tsuda, N. Yamauchi, S. Kitagawa, Anal. Sci. 16 (2000) 847.
[78] T. Tsuda, S. Kitagawa, Y. Yamamoto, Electrophoresis 23 (2002) 2035.
[79] R. Guo, X. Pu, J. Ouyang, X. Li, P. Luo, Y. Yang, Electrophoresis 23 (2002) 1110.
[80] L. He, R.J. Jepsen, L.E. Evans, D.W. Armstrong, Anal. Chem. 75 (2003) 825.
[81] K.M. Fuller, C.F. Duffy, E.A. Arriaga, Electrophoresis 23 (2002) 1571.

[82] A. Strack, C.F. Duffy, M. Malvey, E.A. Arriaga, Anal. Biochem. 294 (2001) 141.
[83] C.F. Duffy, K.M. Fuller, M. Malvey, R. O'Kennedy, E.A. Arriaga, Anal. Chem. 74 (2002) 171.
[84] N. Gunasekera, K. Musier-Forsyth, E.A. Arriaga, Electrophoresis 23 (2002) 2110.
[85] J.R. Philippot, F. Schuber, Liposomes as Basic Tools in Research and Industry, 1995, CRC Press, Boca Raton, FL.
[86] K. Kawakami, Y. Nishihara, K. Hirano, Langmuir 15 (1999) 1893.
[87] S.K. Weidmer, J. Hautala, J.M. Holopainen, P.K.J. Kinnunen, M. Reikkola, Electrophoresis 22 (2001) 1305.
[88] K. Kawakami, Y. Nishihara, K. Hirano, J. Colloid Interf. Sci. 206 (1998) 177.
[89] M.A. Roberts, L. Locascio-Brown, W.A. MacCrehan, R.A. Durst, Anal. Chem. 68 (1996) 3434.
[90] K. Tsukagoshi, H. Akasaka, R. Nakajima, T. Hara, Chem. Lett. 25 (1996) 467–468.
[91] C.F. Duffy, S. Gafoor, D.P. Richards, H. Admadzadeh, R. O'Kennedy, E.A. Arriaga, Anal. Chem. 73 (2001) 1855.
[92] A. Polozova, F.M. Winnik, Langmuir 15 (1999) 4222.
[93] K. Tsukagoshi, Y. Okumura, R. Nakajima, J. Chromatogr. A 813 (1998) 402.
[94] S.P. Radko, M. Statsna, A. Chrambach, Anal. Chem. 72 (2000) 5955.
[95] P.D. Grossman, J.C. Colburn, Capillary Electrophoresis, Theory and Practice, Academic Press, San Diego, CA, 1992, p. 117.
[96] R.W. O'Brien, L.R. White, J. Chem. Soc., Faraday Trans. 77 (1978) 1607.
[97] P.H. Wiersema, A.L. Loeb, J.T.G. Overbeek, J. Colloid Interf. Sci. 22 (1966) 78.